Strojniški vestnik - Journal of Mechanical Engineering 65(2019)9, 495-502

DOI:10.5545/sv-jme.2019.6027 *Original Scientific Paper*
Received for review: 2019-02-07
Received revised form: 2019-06-12
Accepted for publication: 2019-07-12

Selected Microstructural and Mechanical Properties of Open-Cell Metal Foams

Wojciech Depczyński*
Kielce University of Technology, Faculty of Mechatronics and Mechanical Engineering, Poland

The microstructure and mechanical properties of open-cell metal foams have long been studied from various angles. The materials discussed in this paper were fabricated using an unconventional sintering method and their properties are unique. An important part of the process is reduction of Fe(III) oxide, acting as a foaming agent and a space holder. Four powder mixtures were analysed: ASC100.29, ASC100.29 + C, DISTALOY SE and DISTALOY SE + C. The aim of the tests, performed with a specially developed setup, was to determine the impact energy absorption capacity of the Fe-based foams. From the results, it is clear that the metal foams can be used in many applications, including lightweight structures, filters, heat exchangers and energy-absorbing systems.
Keywords: open-cell metal foams, Fe-based foams, reduction of metal oxides, space holder technique, energy dissipation

Highlights
- *The Fe-based metal foams were produced through sintering, which is an efficient and cost-effective process.*
- *The reduction of Fe (III) oxide by hydrogen and the addition of Cu were responsible for a uniform structure and open porosity. The average pore diameter did not exceed 100 μm; the porosity ranged from 67.9 % to 80.3 %, depending on the powder mixture composition.*
- *The motion of the hammer striking the material was monitored using a time-lapse camera.*
- *The Fe-based foams seem suitable for lightweight structures, energy-dissipating and energy-absorbing systems, filters, catalytic converters, and heat exchangers.*

0 INTRODUCTION

Iron has been used as a basic material for everyday tools and weapons since prehistoric times. After the 19th century, which saw the emergence of new technologies for the production of iron-based alloys, steel has become ubiquitous, especially in construction. Now, with dynamic changes in technology, there is a need for new classes of materials that exhibit new characteristics.

Looking for inspiration and solutions to difficult problems, engineers and scientists all over the world have often used nature, the best source of knowledge. For example, Ashby **[1]** wrote, "When modern man builds large load-bearing structures, he uses dense solids: steel, concrete, glass. When nature does the same, she generally uses cellular materials: wood, bone, coral".

Numerous experiments have been carried out to verify concepts concerning the fabrication and application of structural sponge-like materials. Some of the first successful attempts to produce foam materials for structural purposes led to the creation of porous polymer membranes **[2]** and porous polymer electrolytes **[3]**. Much of the research in this area has focused on the fabrication of advanced metal foams **[4]**. Several technologies have been invented to produce metal foams with closed or open porosity, with a crystalline or amorphous structure, and with pores ranging from a micrometre to several millimetres in size **[5]** and **[6]**.

These efforts have resulted in many new applications, e.g. aluminium sound absorbers, copper heat exchangers, and nickel battery electrodes. However, Arwade et al. **[7]** complained, "Steel is one of the most widely used engineering materials, yet today no foam using steel as the base material is commercially available". Further research is thus essential to develop efficient and cost-effective methods to produce Fe-based foam materials with desirable properties **[8]** and **[9]**.

Sintering is one of the cheapest and most efficient methods to fabricate porous iron-based materials. It is not necessary to reach the melting point of iron to obtain a desired structure; porosity is achieved by using a space holder or a foaming agent. Bekoz and Oktay **[10]** fabricated sintered low-alloy steel foams using the space holder-water leaching technique. Their materials had porosity ranging from 47.8 % to 70.9 %, depending on the space holder size (500 μm to 1200 μm). Murakami et al. **[11]** produced iron foams using CO and CO_2 as foaming gases; their maximum porosity was 55 %, and an average pore was 500 μm in size. These processes, however, involved powder compaction, which had a negative effect on the material structure. The sintered porous

*Corr. Author's Address: Kielce University of Technology, Faculty of Mechatronics and Mechanical Engineering, 25-314 Kielce, Poland, wdep@tu.kielce.pl

iron-based material discussed in this article differs from conventionally produced iron foams in that no compaction of powders is applied [12].

The motivation for this project was that there are hardly any studies on the behaviour of open-cell Fe-based foams used as energy absorbers.

1 MATERIALS AND METHODS

The foams to be tested were produced using the sintering method described in Patent PL 199720 B1 [13]. The technology involves adding some oxide easy to reduce by hydrogen to act both as a foaming agent and a space holder. In this study, Fe (III) oxide was employed. Reacting with the atmosphere used during sintering, Fe (III) oxide was reduced to iron by hydrogen from dissociated ammonia to create hollow spaces inside the material.

Another important factor contributing to the production of a cellular structure is the presence of water vapour and CO and/or CO_2. These gases act as foaming agents. Released from the spaces occupied by the sintered powder, they create open interconnected cells. This method has been successfully tested to produce copper foams (Cu + CuO + Cu_2O sintered in a reducing atmosphere of dissociated ammonia) to be used for enhanced heat transfer surfaces in heat exchangers operating in the nucleate boiling mode [14] and [15]. The copper-based foams, being 0.2 mm to 1 mm in thickness, had a porosity of 45 % to 70 %. The open pores ranged from about 50 µm to 100 µm in size. Since very good results were reported for the copper-based foams, research was undertaken to study the use of Fe and its oxides.

2 EXPERIMENT

The compositions of the metal precursors were designed using commercially available powders: Hoganas atomized iron powder ASC100.29, Hoganas diffusion-alloyed powder DISTALOY SE, Chempur iron(III) oxide powder, Poch Norit SX2 carbon powder and Amil copper powder. The four mixtures created were labelled as: ASC100.29, ASC100.29 + C,

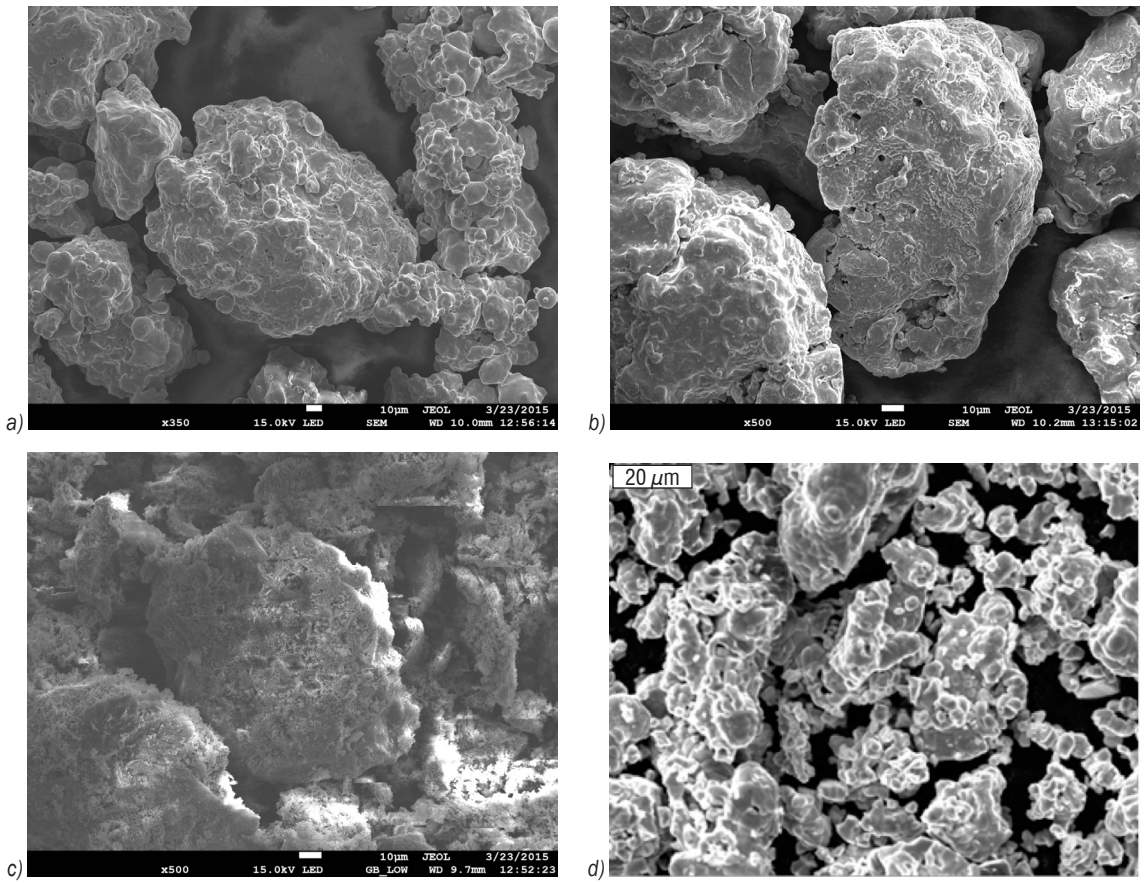

Fig. 1. *SEM images of the constituent powders: a) ASC 100.29, b) DISTALOY SE, c) iron (III) oxide, and d) copper*

DISTALOY SE, and DISTALOY SE + C. All of them had copper added, to act as a diffusion catalyst, and iron (III) oxide, to function as a foaming agent and a space holder. All the mixture constituents were in powder form. The chemical compositions of the iron powders are shown in Table 1. The powder mixtures were not compacted; the particles were only affected by gravity. The shape and dimensions of the dies (steel containers) determined the shape and dimensions of the sintered specimens. The containers measured 30 mm × 50 mm × 100 mm.

Table 1. *Compositions of the iron powders*

Powder	Chemical composition, [%]					
	C	Cu	Ni	Mo	O	Fe
ASC100.29	< 0.01	-	-	-	-	bal
DISTALOY SE	< 0.01	1.5	4	0.5	-	bal

Scanning electron microscopy (SEM) analysis was performed to have a closer look at the size and shape of particles within the constituent powders. Fig. 1 shows the SEM images taken using a JOEL JSM-7100F microscope.

Table 2 provides the percent compositions of the powder mixtures used. To simplify the names of the materials, ASC100.29 will be shortened to ASC, and DISTALOY SE to SE.

Table 2. *Percent compositions of the powder mixtures to be sintered*

Constituents	Powder mixture composition [%]			
	ASC	ASC +C	SE	SE +C
ASC100.29	85	85	-	-
DISTALOY SE	-	-	85	85
Cu	5	4.2	5	4.2
Iron (III) oxide	10	10	10	10
C	-	0.8	-	0.8

The specimens were fabricated by sintering at a temperature of 1130 ºC in a tube furnace. Iron (III) oxide was reduced by hydrogen from dissociated ammonia.

After sintering for 50 minutes, the specimens were placed in the cooling chamber. High temperature and the presence of hydrogen contributed to the reduction of iron (III) oxide. Hollow spaces formed inside the solid structure. The iron (III) oxide reduction was the major factor in the porosity formation. Iron powder particles adhered to one another to form diffusion connections. At 1085 ºC, the copper powder underwent a phase transition process (solid to liquid). The melted copper acted as a reaction catalyst.

3 RESULTS

3.1 Microstructural Characterisation

The foam materials fabricated through sintering in steel containers were tested as energy absorbers. Since Kujime et al. **[16]** reported spark erosion to be the most suitable for cutting porous carbon steel,

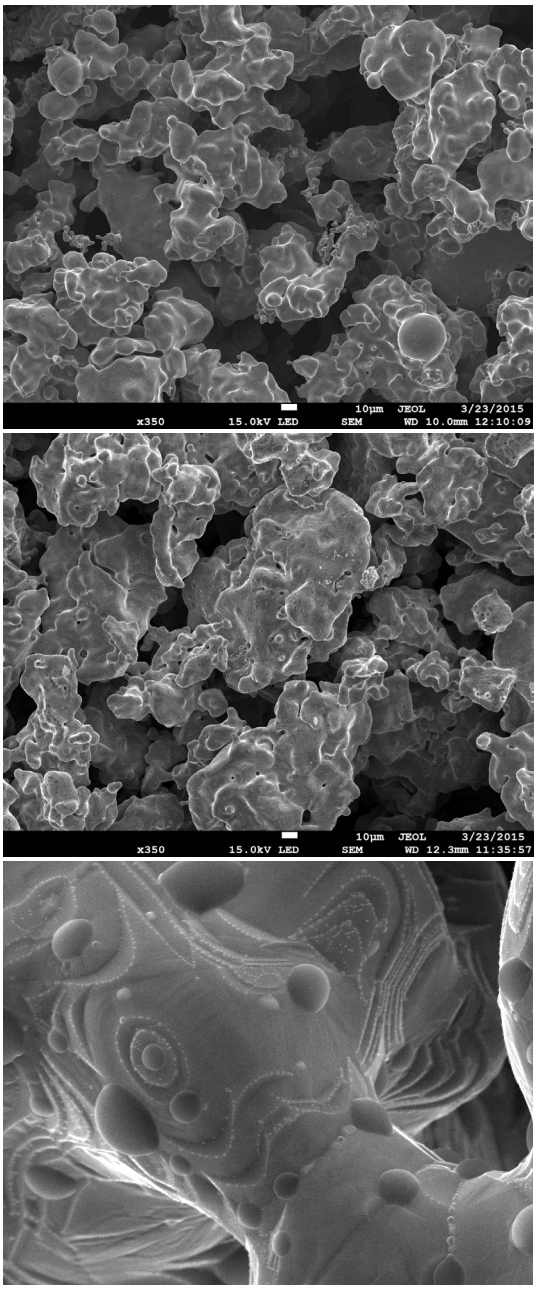

Fig. 2. *SEM images of the sintered iron based powders: a) ASC (magnification 350x) , b) SE (magnification 350x) and c) SE (magnification 5000x), a bridge between particles visible*

this method was selected to prepare the specimens for metallographic examinations. The specimens, 14 mm in thickness and 16 mm in diameter, were geometrically symmetrical. Some of the cross-sectional specimens were etched using Nital to reveal the microstructure of the porous material. Optical (OM) and SEM examinations were used to characterize the foams. An interesting observation during the SEM analysis was that copper in the liquid state initiated formation of diffusion connections between the spherical iron particles. The results can be seen in Fig. 2.

The structure generated in the sintering process was of the open-cell type. Determining the average size of pores was not easy because of their random arrangement. The pore diameter, which was approximately 100 µm, was determined on the basis of OM measurements in longitudinal and cross-sectional planes using Nikon NIS-Element AR imaging software. The Cavalieri-Hacquert principle was employed for the pore size estimation. The reduction of Fe_2O_3, acting as a space holder, greatly contributed to the formation of a network of interconnected open pores. Fig. 2c shows a bridge between two Fe particles being a result of diffusion.

The porosities of the foam materials were determined using optical microscopy. For ASC, ASC + C, SE and SE + C, they were: 67.9, 77.8, 75.7 and 80.3, respectively. Porosity was measured in the longitudinal and cross-sectional planes using NIKON NIS-Elements AR imaging software. Again, the Cavalieri-Hacquert principle was applied.

3.2 Impact Testing

An important mechanical property of porous metal materials is high impact energy absorption capacity. The impact tests were performed using a specially developed setup shown in Fig. 3.

Fig. 3. *The setup for performing impact energy absorption tests*

The experiments consisted in striking a foam-filled steel container using a special hammer with a known mass. The motion of the hammer striking a specimen was monitored using a time-lapse camera (Fig. 4).

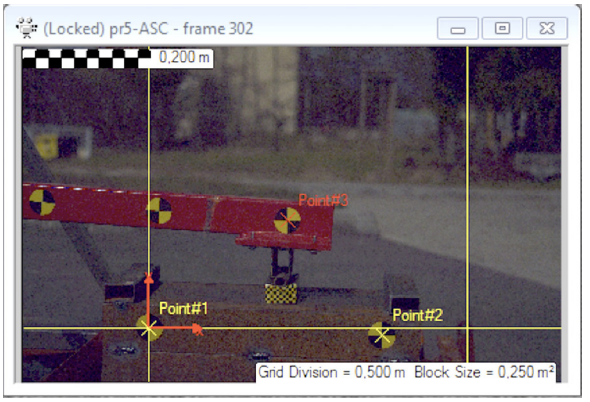

Fig. 4. *Hammer motion analysis using TEMA Motion*

TEMA Motion software was applied to analyse the motion of the moving hammer.

Six specimens were tested. They were all steel containers with different contents. Four were filled with sintered powders: ASC, ASC + C, SE and SE + C (Fig. 5). There were a further two containers tested, one empty and the other filled with sawdust.

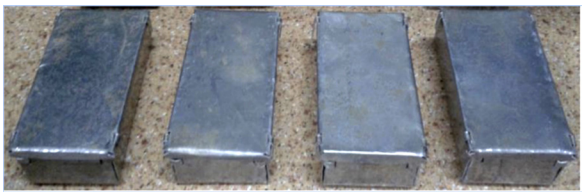

Fig. 5. *The steel containers filled with different iron-based porous materials before the impact tests*

All the tests were conducted under approximately the same conditions. The hammer mass was m = 2.3 kg. Fig. 6 shows the maximum decelerations obtained using the TEMA Motion software.

The TEMA MOTION data were used to determine the hammer deceleration, which was approximately 8000 [m/s²], i.e. 800 G. The speed of the striking hammer was 11 [m/s]. The impact lasted for about 25.5 milliseconds. Then, the hammer bounced off the specimen. The kinetic energy of the impact was 139.15 J. The deformation that the energy absorbers suffered can be seen in Figs. 7 and 8.

The empty container used for calibration was completely destroyed. The same effect was observed for the container with sawdust. The proper specimens, i.e. the containers filled with ASC, ASC + C, SE and SE + C powders were deformed to varying degrees.

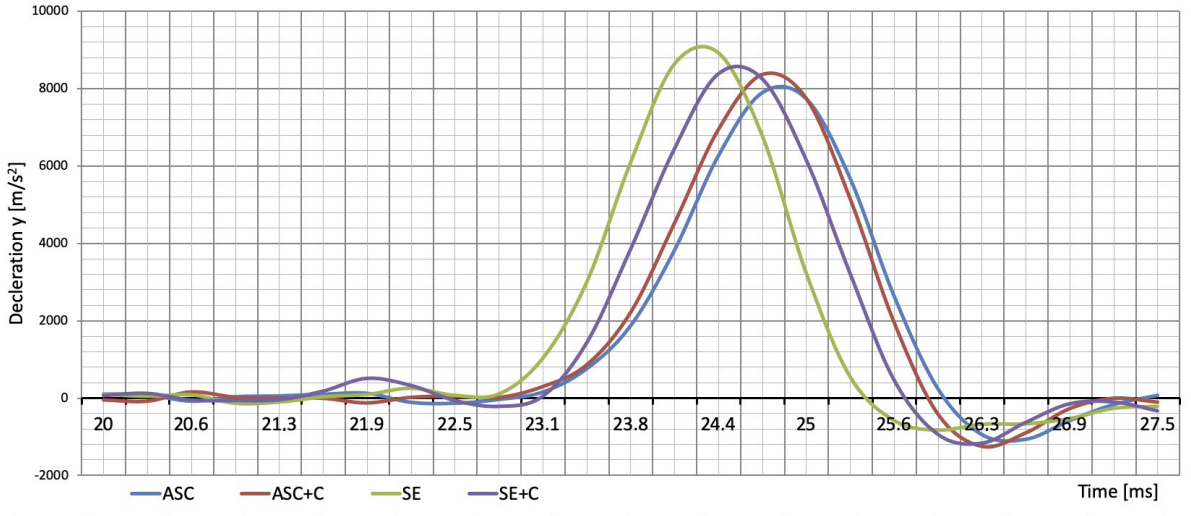

Fig. 6. *Deceleration vs. time for the ASC, ASC + C, SE and SE + C specimens*

Each specimen absorbed a different amount of the kinetic energy of the impact, depending on the filling properties of the foam.

Fig. 7. *Front view of the deformed specimens; from left: four containers filled with foam materials, one filled with sawdust and one empty*

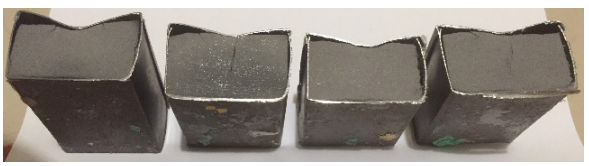

ASC *SE* *ASC+C* *SE+C*

Fig. 8. *Cross sections of the deformed specimens*

The first test was conducted for ASC. During the 25.5 millisecond impact, the hammer came into contact with the test piece for up to 37 milliseconds. This caused a displacement of 0.013 [m]. The displacements measured for the other materials, i.e. ASC + C, SE and SE + C are given in Table 3.

Table 3. *Deformation of the steel containers filled with the porous materials tested*

Absorber	Displacement [m]	Mass [g]
ASC	0.013	443.20
ASC + C	0.008	435.32
SE	0.007	450.84
SE + C	0.009	430.10

4 DISCUSSION

High porosity observed in all the four materials was a combined result of the properly designed powder mixture composition and the optimal sintering conditions. The sintering at 1130 ºC for 50 minutes resulted in a uniform distribution of pores. If a shorter heating time and a lower heating temperature had been used, the reduction of iron (III) oxide would have been insufficient and pore formation retarded. There was no phase transition for iron particles, but they formed a network of interconnected cells. The change of solid copper powder particles into a liquid phase led to an increase in energy at the iron grain boundaries. Copper was also used as the foaming agent producing open interconnected cells.

The findings of Murakami et al. [11] on iron-based porous materials have contributed to a better understanding of the nature of the iron foam formation process involving the occurrence of a semi-liquid phase. The use of 1 % of hematite [Fe_2O_3] as a foaming agent helped produce a material with a maximum porosity of 55 %, where pores ranged from 500 µm to 800 µm in size. When the content of hematite exceeded 1 %, the porosity decreased. Murakami et al. observed, "While the increase in the hematite content increases the amount of foaming gas and consequently the porosity, the excess amount of gas generated by the addition of an excess amount of the foaming agent appears to decrease the porosity. However, the addition of an excess amount of hematite may yield pores with a high pressure in the melt, which may bubble out from the melt" [11]. It is interesting to note

that when hematite was relatively high, i.e. at 2 %, the pore diameters decreased with an increase in porosity. This finding corresponds to the results obtained in this study; the addition of 10 % Fe (III) oxide by volume led to the formation of pores approximately 100 μm in diameter.

The formation of porosity at the macro and micro scales was investigated by Bekoz and Oktay **[10]** for low-alloy steel foams. As they used carbamide as a space holder, macro pores were more than 1000 μm in diameter. The sintering of Hoganas Distaloy AB steel powder at 1200 ºC for 60 minutes contributed to the formation of micropores with a diameter of less than 100 μm. The sintering conditions were very similar to those discussed in this article. It is possible, however, that the micro porosity obtained by Bekoz and Oktay **[10]** was a side effect of the application of carbamide as a space holder.

Internal porosity can be developed in a number of ways. Kujime et al. **[16]**, for example, applied the gas entrapment method, which involved supplying pressurized hydrogen and helium to a melted metal to produce porous carbon steel with a porosity of 26 % to 44 % and a pore diameter of 500 μm to 700 μm. Compared with the materials described in this article, their lotus-type foams had a structure with larger pores and lower porosity. The gas blowing method they employed differed from the conventional techniques of porosity formation. It can thus be concluded that the porosity of the lotus-type steel foam increases with increasing partial pressure of hydrogen gas **[16]**.

Another important factor that defines a porous structure is the gas pressure exerted on the material during the sintering process. Saadatfar et al. **[17]** studied the influence of air overpressure on the porosity level using X-ray micro-computed tomography (micro-CT) for non Fe-based metal foams All the specimens analysed in this paper were prepared under a pressure of 1 bar. In his earlier paper **[18]**, the author provides the micro-CT results obtained for similarly fabricated Cu-based foams, where the foaming agent is copper oxide.

The optical microscopy was very useful for determining the percent porosities and pore diameters, but it was not sufficiently accurate to characterize the foam microstructures and, accordingly, the pore formation process. SEM was a suitable method to analyse foam structures in more detail. Maire et al. **[19]** remark, "The complex 3D architecture of solid foams requires observation techniques permitting a high depth of field. Amongst the standard available techniques, only SEM shows enough depth of focus to apprehend the structure of these materials". The author of this article successfully modelled the structures of similar foams and compared them with SEM images, as described in **[20]**.

Uniform porosity observed in the foams described in this article was a result of two main factors: mechanical mixing of powders and reduction of iron (III) oxide at constant temperature during sintering. By contrast, Rabei et al. **[21]**, who deal with iron-based porous structures applied pre-sintering vibration, which led to considerable differences in porosity between the powder matrix and the hollow spheres embedded in it. The vibration caused part of the powder to adhere to the sphere walls with the rest forming uncompacted matrix.

Applications of metal foams include energy absorbers. Research in this area has involved experiments as well as modelling and simulation **[22]** to **[24]**. The empirical data concerning the impact energy absorption capacity of the four foams analyzed in this paper seem promising. The highest values were reported for the ASC foam, while the lowest for SE. Thus, the ASC specimen was the most deformed and the SE the least. Also, the SE foam had the lowest porosity because of the highest mass. The ASC+C and SE +C specimens exhibited similar energy absorption performance, worse than ASC and better than SE, respectively. In all the cases, deformation was directly dependent on the hammer deceleration. The presence of carbon in the powder mixtures resulted in higher porosity of the foams. When added to SE, it improved its energy dissipation efficiency. On the other hand, the addition of carbon to ASC caused a slight decrease in the material energy absorption performance, which was due to changes in the strength of diffusion connections between iron particles. As carburization occurred, an increase in the carbon content improved the strength properties of this material (ASC + C).

From the deformation behaviour of the materials tested, it is apparent that they had a potential to absorb more energy. As they were fabricated through powder metallurgy, their parameters, which are dependent on the powder mixture composition, are easy to control.

There are no standards for energy absorption measurement and then interpretation of results obtained for open-cell, closed-cell or syntactic metal foams, which makes the comparison of impact test data difficult. Results from static tests, such as quasi-static compression tests, are more comparable **[25]** to **[27]**. The results of the dynamic tests described in this paper were obtained at a relatively small energy impact of less than 140 J, which resulted from the test setup design. Drop-weight (Pellini) tests would have provided more accurate data.

5 CONCLUSIONS

This paper has dealt with a powder metallurgy method of preparing open-cell metal-foams. Sintering processes are much more energy-efficient and cheaper than other techniques used to produce porous metal materials. The Fe-based foams tested had structures that are controllable to some extent. Their porosity depended on the composition of the powder mixture, and thus indirectly on the size and shape of grains. The chemical compositions of the materials to be sintered were carefully designed to ensure proper filling of the steel die.

The metal foams were characterized using optical and SEM analysis. Both techniques are suitable to determine the differences in microstructure. Porosity was largely dependent on the powder mixture composition. The presence of alloying elements may have been the reason for higher porosity of the sintered materials. As the phenomenon is not easy to explain, there is a need for further research in this area.

The tests performed with a specially developed setup showed that the Fe-based metal foams had high impact energy absorption capacity because of their high porosity. The relationship between these two properties should be further investigated.

Materials with similar porosity, e.g. ones with a lotus-type structure have so far been fabricated through technologies involving a liquid-phase, which is far more expensive than the method described here.

Open-cell Fe-based foams produced in this way are likely to be used in applications including lightweight structures, energy-dissipating and energy-absorbing systems filters, catalytic converters and heat exchangers.

6 ACKNOWLEDGMENTS

Special thanks to dr hab. inż. Marek Jaśkiewicz and other staff members of the Department of Automotive Engineering and Transport at the Faculty of Mechatronics and Mechanical Engineering of the Kielce University of Technology, for access to their laboratory and their assistance during the tests.

7 REFERENCES

[1] Ashby, M.F. (1983). The mechanical properties of cellular solids. *Metallurgical Transactions: A*, vol. 14, no. 9, p. 1755-1769, **DOI:10.1007/BF02645546**.

[2] van de Witte, P., Dijkstra, P.J., van den Berg, J.W.A., Feijen, J. (1996). Phase separation processes in polymer solutions in relation to membrane formation. *Journal of Membrane Science*, vol. 117, no. 1-2, p. 1-31, **DOI:10.1016/0376-7388(96)00088-9**.

[3] Cao, J.-H., Zhu, B-K. Xu, Y.-Y. (2006). Structure and ionic conductivity of porous polymer electrolytes based on PVDF-HFP copolymer membranes. *Journal of Membrane Science*, vol. 281, no. 1-2, p. 446-453, **DOI:10.1016/j.memsci.2006.04.013**.

[4] Banhart, J. (2013). Light-metal foams—History of innovation and technological challenges. Advanced Engineering Materials, vol. 15, no. 3, **DOI:10.1002/adem.201200217**.

[5] Oriňáková, R., Andrej Oriňák, A., Markušová Bučková, L., Giretová, M., Medvecký, L., Evelína Labbanczová, E., Kupková, M., Monika Hrubovčáková, M., Koval, K. (2013). Iron based degradable foam structures for potential orthopedic applications. *International Journal of Electrochemical Science*, vol. 8, p. 12451-12465, **DOI:10.1515/pmp-2016-0008**.

[6] Brothers, A.H., Scheunemann, R., DeFouw, J.D., Dunand, D.C. (2005). Processing and structure of open-celled amorphous metal foams. *Scripta Materialia*, vol. 52, no. 4, p. 335-339, **DOI:10.1016/j.scriptamat.2004.10.002**.

[7] Arwade, R.S., & Hajjar, J., Schafer, B., Moradi, M., Smith, B., Szyniszewski, S. (2011). Steel foam material processing, properties, and potential structural applications. *Structural Materials and Mechanics, Proceedings of the NSF Engineering Research and Innovation Conference*, **DOI:10.1016/j.jcsr.2011.10.028**.

[8] Mutulu, I., Oktay, E. (2011). Processing and properties of highly porous 17-4 PH stainless steel. *Powder Metallurgy and Metal Ceramics*, vol. 50, no. 1-2, p. 73-82, **DOI:10.1007/s11106-011-9305-1**.

[9] Jee, C.S.Y., Guo, Z.X., Evans, J.R.G., Özgüven, N. (2000). Preparation of high porosity metal foams. *Metallurgical and Materials Transactions B*, vol. 31, no. 6, p. 1345-1352, **DOI:10.1007/s11663-000-0021-3**.

[10] Bekoz, N., Oktay, E. (2013). Mechanical properties of low alloy steel foams: Dependency on porosity and pore size. *Materials Science and Engineering: A*, vol. 576, p. 82-90, **DOI:10.1016/j.msea.2013.04.009**.

[11] Murakami, T., Ohara, K., Narushima, T., Ouchi, C. (2007). Development of a new method for manufacturing iron foam using gasses generated by reduction of iron oxide. *Materials Transactions*, vol. 48, no. 11, p. 2937–2944, **DOI:10.2320/matertrans.MRA2007127**.

[12] Park, C., Nutt, S.R. (2001). Effects of process parameters on steel foam synthesis. *Materials Science and Engineering: A*, vol. 297, no. 1-2, p. 62-68, **DOI:10.1016/S0921-5093(00)01265-X**.

[13] Żórawski, W., Chatys, R., Depczyński, W. (2008). *A Method for Producing Porous Structures, Patent PL 199720 B1*, Patent Office of the Republic of Poland, Warszawa. (in Polish)

[14] Depczyński, W. (2014). Sintering of copper layers with a controlled porous structure. METAL *23rd International Conference on Metallurgy and Materials*, p. 1219-1224.

[15] Wójcik, T.M. (2012). Heat transfer enhancement and surface thermo stabilization for pool boiling on porous structures. *EPJ Web of Conferences, Experimental Fluid Mechanics*, vol. 25, art. no. 01100, **DOI: 10.1051/epjconf/20122501100**.

[16] Kujime, T., Hyun, S.-K., Nakajima, H. (2006). Fabrication of lotus – type porous carbon steel by the continuous zone melting and its mechanical properties. *Metallurgical and Materials Transactions A*, vol. 37, no. 2, p. 393–398, **DOI:10.1007/s11661-006-0009-y**.

[17] Saadatfar, M., Garcia-Moreno, F., Hutzler, S., Sheppard, A.P., Knackstedt, M.A., Banhart, J., Weaire, D. (2009). Imaging of metallic foams using X-ray micro-CT. *Colloids and Surfaces A: Physicochemical and Engineering Aspects*, vol. 344, no. 1-3, p. 107-012, **DOI:10.1016/j.colsurfa.2009.01.008**.

[18] Depczyński, W. (2014). Investigating porosity of sintering porous copper structure with 3D micro-focus X-ray computed tomography (μCT). *Journal of Achievements in Materials and Manufacturing Engineering*, vol. 66, no. 2, p. 67-72.

[19] Maire, É, Adrien, J., Petit, C. (2014). Structural characterization of solid foams. *Comptes Rendus Physique*, vol. 15, no. 8-9, p. 674-682, **DOI:10.1016/j.crhy.2014.09.001**.

[20] Depczyński, W., Kazała, R., Ludwinek, K., Jedynak, K. (2016). Modelling and Microstructural characterization of sintered metallic porous materials. *Materials*, vol. 9, no. 7, art. no. 567, **DOI:10.3390/ma9070567**.

[21] Rabei, A., Vendra, L., Reese, N., Young, N., Neville, B.P. (2006). Processing and characterization of a new composite metal foam. *Materials Transactions*, vol. 47, no. 9, p. 2148–2153, **DOI:10.2320/matertrans.47.2148**.

[22] Marx, J., Portanova, M., Rabiei, A. (2018). A study on blast and fragment resistance of composite metal foams through experimental and modeling approaches. *Composite Structures*, vol. 194, p. 652-661, **DOI:10.1016/j.compstruct.2018.03.075**.

[23] Garcia-Avila, M., Portanova, M., Rabiej, A. (2014). Ballistic performance of a composite metal foam-ceramic armor system. *Procedia Materials Science*, vol. 4, p. 151-156, **DOI:10.1016/j.mspro.2014.07.571**.

[24] Garcia-Avila, M., Portanova, M. Rabiej, A. (2015). Ballistic performance of a composite metal foam. *Composite Structures*, vol. 125, p. 202-211, **DOI:10.1016/j.compstruct.2015.01.031**.

[25] Depczynski, W., Miłek, T., Nowakowski, Ł. (2017). Experimental comparison between upsetting characteristics of porous components prepared by Fe-based sintering technology. *IOP Conference Series-Materials Science and Engineering*, vol. 179, art. no. 012015, **DOI:10.1088/1757-899X/179/1/012015**.

[26] Rabiei, A., Garcia-Avila, M. (2013). Effect of Various parameters on properties of composite steel foams under variety of loading rates. *Materials Science & Engineering: A*, vol. 564, p. 539-547, **DOI:10.1016/j.msea.2012.11.108**.

[27] Alvandi-Tabrizi, Y., Whisler, D.A., Kim, H., Rabiei, A. (2015). High strain rate behavior of composite metal foams. *Materials Science and Engineering: A*, vol. 631, p. 248-257, **DOI:10.1016/j.msea.2015.02.027**.